References

[1]Panda, J., "Wide Angle Light Scattering in Shock-Laser Interaction," *AIAA Journal*, Vol. 33, No. 12, pp. 2429–2431.

[2]Panda, J., "Partial Spreading of a Laser Beam into a Light Sheet by Shock Waves and Its Use as a Shock Detection Technique," NASA CR-195329, May 1994.

[3]Lassiter, L. W., and Hubbard, H. H., "The Near Noise Field of Static Jets and Some Model Studies of Devices for Noise Reduction," NACA TN 3187, July 1954.

[4]Norum, T. D., and Seiner, J. M., "Location and Propagation of Shock Associated Noise from Supersonic Jets," AIAA Paper 80-0983, June 1980.

Stress and Failure Analysis for Cross-Plied Curved Composite Laminates

Naoyuki Watanabe*
Tokyo Metropolitan Institute of Technology, Tokyo 191, Japan
and
Takao Okada†
National Aerospace Laboratory, Tokyo 182, Japan

I. Introduction

MANY laminated composite structures that have a curved portion, such as an angle bracket, a co-curved web, or a frame, are used for aerospace structures,[1] because design requirements often necessitate the use of complex geometries in the fabrication of load-bearing components. In such curved portions, a tensile radial stress happens under some loading conditions.[2–4] In the curved region of a laminated structure, two major modes of failure were observed, i.e., transverse matrix cracking due to bending stress and interlaminar delamination due to high interlaminar normal stress in the thickness direction. If delamination occurs first, then a total failure, i.e., final failure, of the structure results. However, the structure usually can sustain additional loading after initial transverse matrix cracking. Under increasing loading, these matrix cracks would cause delaminations that would lead to the total collapse of the structure.[2,4,5] Thus, a delamination between layers may be caused by the interlaminar normal stress in the middle region of such laminate far from its free edge, whereas in a flat laminate it always begins to expand necessarily from a free edge. Therefore, for investigating the strength of curved laminates the radial stress must be evaluated accurately.

In this paper, cross-plied curved composite laminates are analyzed for stress and failure using the two-dimensional finite element method (FEM). The strength for in-plane failure of each layer is predicted using the Tsai–Wu criterion, and the maximum radial stress criterion is used for a delamination. These two strengths are investigated for various lay-ups. The three-dimensional FEM is carried out for indicating the validity of the two-dimensional FEM.

II. Effect of Stacking Sequence on the Strength of Cross-Plied Curved Composite Laminate

The effect of the stacking sequence on the strength of cross-plied curved composite laminates shown in Fig. 1 is evaluated. Plane stress state on the x–y plane is assumed and the two-dimensional FEM is carried out. The material constants, the strength properties, and the dimensional parameters are assumed here as follows:

$$L_p = 10\text{ mm},\quad L_h = 10\text{ mm},\quad R_0 = 8\text{ mm}$$
$$R_i = 5\text{ mm},\quad t = 3\text{ mm},\quad E_L = 140\text{ GPa},\quad E_T = 11\text{ GPa}$$
$$G_{LT} = 5.84\text{ GPa},\quad G_{TT} = 4.44\text{ GPa},\quad \upsilon_{LT} = 0.3$$
$$\upsilon_{TT} = 0.28,\quad F_{Lt} = 1.50\text{ GPa},\quad F_{Lc} = 1.00\text{ GPa}$$
$$F_{Tt} = 0.0685\text{ GPa},\quad F_{Tc} = 0.194\text{ GPa},\quad F_{LT} = 0.115\text{ GPa}$$

One of the strengths is concerned with the in-plane failure of each layer, and it is assumed to be estimated by means of the Tsai–Wu criterion.[6,7] The coefficient F_{12}^* used in it is assumed to be -0.5 according to Ref. 10. The other strength is related to the delamination on the interface between two adjacent layers and is estimated as follows:

$$\sigma_r \geq F_{Tt} \tag{1}$$

Although the delamination strength isn't the same for each interface of 0/0, 0/90, and 90/90 deg, the exact values are not known, so the preceding assumption is done in this paper also.[2,5] As typical stacking sequence, six are carried out

$$\text{L1: } [0_4/90_3/0_5]_{\text{sym}},\quad \text{L2: } [0_7/90_3/0_2]_{\text{sym}},\quad \text{L3: } [0_2/90_3/0_7]_{\text{sym}}$$
$$\text{L4: } [0_9/90_3]_{\text{sym}},\quad \text{L5: } [0_2/90_{10}]_{\text{sym}},\quad \text{L6: } [0_4/90_3/0_6/90_3/0_8]$$

where the stacking sequence is written from its inside and the 0-deg layer means that fibers go on the x–y plane along its arc and the 90-deg layer means that they go along the out-of-plane direction, i.e., z direction.

Table 1 shows the results under the upward external load. The magnitude of the load when the failure mode begins to occur, the angle of circular arc, and the layer number of the location where the failure occurs are shown in the table. For delamination, the location of the interface is written.

From comparing L1 with L2, it is shown that the shift of 90-deg plies to the middle increases the in-plane failure strength with a

Table 1 Failure loads for in-plane failure and interlaminar delamination together with location where its failure occurs under upward external load for various lay-ups

	In-plane failure			Delamination		
		Location			Location	
Lay-up	Load, N/mm	Angle, deg	Layer[a]	Load, N/mm	Angle, deg	Interface[b]
L1	44.0	15	5 (90)	61.1	25	10 (0), 11 (0)
L2	48.2	25	8 (90)	58.1	19	7 (0), 8 (90)
L3	39.7	15	3 (90)	56.5	25	10 (0), 11 (0)
L4	51.6	25	10 (90)	58.3	19	9 (0), 10 (90)
L5	31.2	15	3 (90)	64.9	15	3 (90), 4 (90)
L6	45.5	15	5 (90)	62.4	25	10 (0), 11 (0)

[a]Number of layers from its inside, and the figure in parentheses indicates the fiber angle.
[b]Interface between two layers.

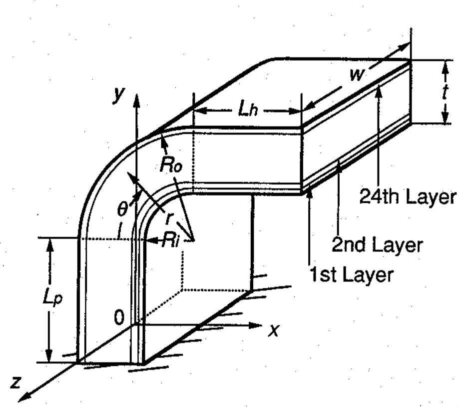

Fig. 1 Cross-plied laminate with a quarter of circular arc.

Presented as Paper 93-1519 at the AIAA/ASME/ASCE/AHS/ASC 34th Structures, Structural Dynamics, and Materials Conference, La Jolla, CA, April 19–22, 1993; received Dec. 14, 1993; revision received March 20, 1995; accepted for publication Aug. 10, 1995.

*Associate Professor, Department of Aerospace Engineering, 6-6, Asahigaoka, Hino-Shi. Member AIAA.

†Researcher, Structural Mechanics Division, 7-44-1, Jindaiji Higashimachi, Chofu-shi.

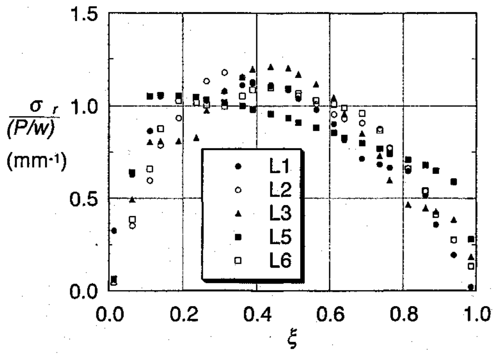

Fig. 2 Comparison on distribution of radial stress σ_r through thickness at the location where a delamination is predicted to occur under upward external load.

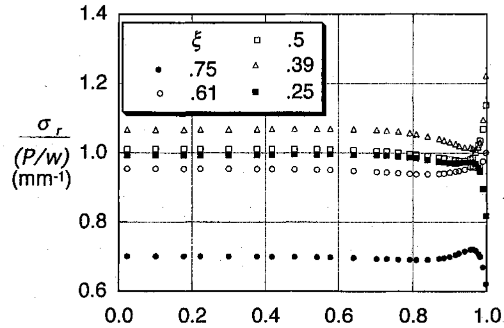

Fig. 3 Distribution of the normal interlaminar stress σ_r with ζ as a parameter of the radial location ξ on the plane of $\theta = 45$ deg, where $\zeta = z/(w/2)$ and $\xi = (r - R_i)/t$.

decrease of the delamination strength. The broken layer is the most inner 90-deg ply in both lay-ups. The location of the delamination is the interface between inner 0-deg plies for L1 but is the interface between the most inner 90-deg ply and its just outer 0-deg ply for L2. The shift to the opposite direction reduces both the in-plane and delamination strengths as comparing L3 with L1. Comparison of L1 with L5 indicates that the addition of 90-deg ply with a reduction of 0-deg ply increases the delamination strength with a considerably large decrease of the in-plane failure strength. The broken layer for L5 is the most inner 90-deg ply, that is the same case as L1. The completely reverse phenomenon to L5 happens for L4. From the comparison of L1 with the unsymmetric lay-up L6, the shift of neutral surface to the outer direction can increase both strengths. The location of the failure is similar to that for L1.

Figure 2 shows the distribution of radial stress σ_r through the thickness where the delamination is predicted to occur for each lay-up. It is noted that the inspected radial location is different from one another; for example, the angle is 25 deg for L1 and 19 deg for L2. It is indicated that the change of the stress is large in the 0-deg ply and small in the 90-deg ply. Because there is no 0-deg ply in the middle section for L5, there is no increase of σ_r, and thus the delamination strength is considered to increase. Contrarily, L2 and L3 have 0-deg plies at the region where σ_r becomes large, and so σ_r becomes larger there. These facts are fairly consistent with the delamination strength as shown in Table 1.

Under the rightward external load, because σ_r is very small under this loading, the delamination strength is far larger than that under the upper one, and the in-plane failure is predicted to occur at the joint between the curved portion and the vertical flat laminate. Under the downward external load, a delamination cannot occur because σ_r is negative everywhere in a curved portion. The result for the leftward external load is similar to the result for the upward load. Therefore, these results are not shown here.

III. Three-Dimensional Stress Analysis

It is well known that the interlaminar stresses come to occur near a free edge of a flat laminate, and the region where those interlaminar stresses are dominant compared with in-plane stresses is limited to the region within the distance of the total laminate thickness from the free edge. For the cross-plied laminate, τ_{yz} and σ_z are the only nonzero interlaminar stresses.[8,9] On the other hand, for a curved laminate the distribution of the interlaminar stresses has not been investigated yet. If the similar fact that they are limited to the small boundary region of the curved laminate is not proven, the results by the two-dimensional analysis come to be only partly meaningful. Therefore, the three-dimensional analysis is carried out, and the stress distribution of the curved cross-plied laminates is evaluated.

The cross-plied laminate with a quarter of circular arc shown in Fig. 1 is analyzed, where the dimensional parameters are the same as those in Sec. II, and the width w is assumed to be 25 mm. The analysis is carried out for the simplest lay-up, L4. The analysis is executed for the half-part of it because of its symmetry to the plane of $z = 0$. Figure 3 shows the normal interlaminar stress σ_r with z coordinate as a parameter of the location of the radial direction on the plane of $\theta = 45$ deg. The abscissa is the normalized distance of z direction, $\zeta = z/(w/2)$, and the ordinate is the normalized stress. The parameter $\xi = (r - R_i)/t$ indicates the normalized radial distance from its inside. In Fig. 3, σ_r is nearly constant within $\zeta = 0.76$, that is, the distance of the laminate thickness from the free edge and is perfectly the same as the two-dimensional FEM analysis. The region where the distribution changes prominently is only outside from $\zeta = 0.95$ for all ξ. The interesting fact is that σ_r of the 90-deg ply increases and the one of 0-deg ply decreases near the free edge.

The magnitude of τ_{rz} is lower approximately by one order than σ_r; τ_{rz} is kept nearly zero in the center region and begins to increase at about $\zeta = 0.6$ and continues to increase. And it decreases abruptly near the free edge. The other interlaminar stress $\tau_{r\theta}$ has the same order as τ_{rz} and the similar tendency to σ_r. These results are not shown here. These facts are consistent with the flat cross-plied laminate.

Consequently, the results of the two-dimensional analysis are considered sufficiently accurate almost all over the curved laminate except for the very small region near the free edge.

IV. Conclusions

Cross-plied curved composite laminates are analyzed for stress and failure. They have two major modes of failure, in-plane failure and interlaminar delamination. The effect of stacking sequence on the strength of cross-plied curved composite laminates is evaluated considering the distribution of radial stress by the two-dimensional FEM. The strength for in-plane failure of each layer is predicted using the Tsai–Wu criterion, and the maximum radial stress criterion is used for a delamination. It is shown that the simultaneous increase of these two strengths should be possible by the following ways: 1) the shift of the 90-deg ply to the middle and 2) the shift of the neutral surface of the laminate to the outer direction. The three-dimensional FEM is carried out at the same time, and the validity of the two-dimensional analysis is verified except for the very small region near the free edge of curved laminates.

Acknowledgment

This research was supported by an internal grant from Tokyo Metropolitan Institute of Technology.

References

[1] Kedward, K. T., Wilson, R. S., and McLean, S. K., "Flexure of Simply Curved Composite Shape," *Composites*, Vol. 20, No. 6, 1989, pp. 527–536.

[2] Martin, R. H., and Jackson, W. C., "Damage Prediction in Cross-Plied Curved Composite Laminates," NASA TM-104089, July 1991.

[3] Chang, F. K., and Springer, G. S., "The Strengths of Fiber Reinforced Composite Bends," *Journal of Composite Materials*, Vol. 20, Jan. 1986, pp. 30–45.

[4] Sun, C. T., and Kelly, S. R., "Failure in Composite Angle Structure Part I: Initial Failure," *Journal of Reinforced Plastics and Composites*, Vol. 7, May 1988, pp. 220–232.

[5] Sun, C. T., and Kelly, S. R., "Failure in Composite Angle Structure Part II: Onset of Delamination," *Journal of Reinforced Plastics and Composites*, Vol. 7, May 1988, pp. 233–244.

[6]Tsai, S. W., and Wu, E. M., "A General Theory of Strength for Anisotropic Materials," *Journal of Composite Materials*, Vol. 5, Jan. 1971, pp. 58–80.

[7]Tsai, S. W., and Hahn, H. T., *Introduction to Composite Materials*, Technomic, Westport, CT, 1980.

[8]Jones, R. M., *Mechanics of Composite Materials*, Hemisphere, New York, 1975.

[9]Wang, J. T. S., and Dickson, J. N., "Interlaminar Stresses in Symmetric Composite Laminates," *Journal of Composite Materials*, Vol. 12, Oct. 1978, pp. 390–402.

Analysis of Thick Multilayered Anisotropic Plates by a Higher Order Plate Element

Marco Di Sciuva* and Ugo Icardi†
Politecnico di Torino, 10129 Turin, Italy

I. Introduction

IN two-dimensional approaches, laminated anisotropic plates and shells have been extensively studied by means of the classical lamination plate theory (CLPT) and the first-order shear deformation theory (FSDT).

The fact that some important modes of failure are related to interlaminar stresses motivated researchers to search for higher order modeling approaches that will serve the purpose of giving predictions of acceptable accuracy and at the same time will be capable of being implemented in practice.

In the literature are found a number of higher order shear deformable models; these models can be grouped into three categories[1] as follows. 1) Approaches based on an assumed global (i.e., for the whole laminate) nonlinear distribution along the thickness of the in-plane displacements or the transverse shearing stresses (smeared laminate models). Since the power expansions in the x_3 coordinate belong to the C^1 class of functions at least (continuity of functions and their first derivative), incompatible transverse stresses appear at interfaces of adjacent layers if the layers have different mechanical properties. 2) Approaches based on an assumed piecewise displacement or stress distribution in the thickness direction (discrete-layer models). Most of the models of this class impose continuity conditions as constraint conditions on each layer, resulting in the number of governing equations increasing with the number of layers in the laminate. 3) Zig-zag models based on piecewise linear or nonlinear through-the-thickness displacement distributions having discontinuous derivatives to allow for appropriate jumps in the strain and stress using the same number of displacement variables as in the corresponding smeared laminate models. In the following we will be interested in the zig-zag models. Specifically, we will make reference to the general formulation recently given by Di Sciuva.[2] The development of shear deformable, multilayered anisotropic plate finite elements follows the same path as in the analytical modeling approaches. For a review of the extensive bibliography on the subject, see the references quoted in Refs. 3–5. In effect, as a basis for the formulation of plate elements of this type, many investigators have employed the smeared laminate models, whereas others make use of the discrete-layer models. In the first approach, the multilayered anisotropic plate element is reduced to an equivalent single anisotropic layer element. Many of the finite element formulations belonging to the second group make use of at least one solid or plate element per layer in the thickness direction. Then this approach requires numerous unknowns, and as a consequence, these formulations become nontractable in the solution of practical engineering problems. The multilayered anisotropic plate finite elements formulated on the basis of the zig-zag plate models overcome this drawback because the number of nodal parameters is independent of the number of layers.[3,5]

Based on the refined third-order zig-zag plate model, Di Sciuva et al.[4] recently formulated an eight-noded general quadrilateral plate element with 56 degrees of freedom (DOF): 10 DOF of the corner nodes (the two in-plane displacements, the two shear rotations, the transverse displacement and its first and second derivatives) and 4 DOF per midside node (the two in-plane displacements and the two shear rotations). Thus, this plate element is characterized by a quadratic variation of the in-plane displacements and shear rotations and quintic variation of the transverse displacement in the element. Only preliminary numerical results were given in Ref. 4. The purpose of the present Note is twofold: 1) to give a brief review of a recent generalization of the zig-zag approach to anisotropic multilayered plates of general lay-ups and 2) to further substantiate the accuracy of the developed eight-noded, curvilinear quadrilateral plate element. To this end, finite element solutions for thickness distribution of transverse shear stresses are compared with analytical results from three-dimensional elasticity and other approximate two-dimensional plate models. The numerical investigations performed in previous works and in the present one reveal the superiority of the zig-zag approaches on the other approximate bidimensional models.

II. Multilayered Plate Model

We consider a plate of constant thickness h made of N parallel thin layers of anisotropic materials perfectly bonded together. The thickness of each layer is assumed to be constant and the material to possess a plane of elastic symmetry parallel to the plate reference surface Ω. Material properties and thickness of each layer may be entirely different. Let x_α be a rectangular Cartesian frame[1] on Ω, x_3 being the normal to Ω. (In this Note, if not otherwise specified, the Einsteinian summation convention over repeated indices will be adopted with Latin indices ranging from 1 to 3 and Greek indices ranging from 1 to 2.) In developing a multilayered plate model that fulfills the contact conditions on the transverse shearing stresses, we assume the following displacement field[2] (in developing the plate model, we assume $\sigma_{33} = 0$):

$$\tilde{u}_\alpha(x_j) = u_\alpha(x_j) + U_\alpha(x_j); \qquad \tilde{u}_3(x_j) = u_3^{(0)}(x_\beta) \tag{1}$$

where

$$u_\alpha(x_j) = \sum_{r=0}^{R} L^{(r)}(x_3)u_\alpha^{(r)}(x_\beta) \tag{2}$$

gives the contribution to the in-plane displacement that is continuous with its derivatives with respect to x_3 (this is the classical expansion used in the smeared laminate models);

$$U_\alpha(x_j) = \sum_{k=1}^{N-1} \phi_\alpha^{(k)}(x_\beta)\left[x_3 - x_3^{(k)}\right]H_k \tag{3}$$

gives the contribution to the in-plane displacement that is continuous with respect to x_3, but with jumps in the first derivative at the interfaces between adjacent layers. Here, $H_k = H[x_3 - x_3^{(k)}]$ is the Heaviside unit function and $\phi_\alpha^{(k)}(x_\beta)$ are functions to be determined by satisfying the contact conditions on the transverse shearing stresses at the interfaces. The details of the derivation are given in Di Sciuva.[2] The functions $L^{(r)}(x_3)$ can be given by any set of linearly independent functions, with at least continuous first derivatives with respect to x_3.

As discussed by Di Sciuva,[2] many multilayered plate models proposed in the literature can be obtained as special cases of the previous one. Here we will focus our attention on symmetric laminated plates in bending. For these plates, let the reference surface

Received Oct. 11, 1994; revision received May 5, 1995; accepted for publication Aug. 10, 1995.

*Associate Professor, Department of Aerospace Engineering, Corso Duca degli Abruzzi, 24.

†Senior Researcher, Department of Aerospace Engineering, Corso Duca degli Abruzzi, 24.